7 Orientational relaxation of $HDO:D_2O$ as an activated process

The orientational relaxation of HDO molecules dissolved in liquid D_2O is studied with polarization-resolved pump–probe experiments. The excitation of the OH stretch vibration is used as a label in order to follow the orientational motion of the HDO molecules in time. The decay of the anisotropy is nonexponential with a typical time scale of 1 ps and can be described with a model involving both a reorientation rate that depends on the OH stretch frequency and spectral diffusion. The dependencies of the anisotropy decay on frequency and temperature provide information on the activation energy for reorientation. This activation energy increases with the hydrogen bond strength.

7.1 Introduction

Orientational diffusion of water molecules is likely to be related to hydrogen-bond breaking and formation, since a hydrogen bond is directional, i.e. the O–H···O group is approximately linear.[75] The orientation vector of a particle that is subject to orientational diffusion changes by 1 rad typically in a time $3\tau_r$, where τ_r is the orientational correlation time. (See §7.6.1 for an exact definition.) Already in 1929, Debye[2,22] used the viscosity $\eta \approx 10^{-3}$ Pa·s of water and the radius $a \approx 2$ Å of a water molecule for the estimate

$$\tau_1 = 3\tau_r = \frac{4\pi a^3 \eta}{k_B T} = 25 \text{ ps}, \tag{7.1}$$

at $T = 293$ K. This equation is now known as the Debye-Stokes-Einstein equation. Debye formulated a theory that relates the time constant τ_1 (now known as the Debye time) to the dependence of the dielectric constant ϵ of a liquid medium on frequency ω,

$$\epsilon(\omega) = \epsilon(\infty) + \frac{c}{1 - i\omega\tau_1}. \tag{7.2}$$

From the dielectric properties in the microwave (GHz) range, τ_1 can be estimated to be 8.1 ps, as mentioned by Bloembergen in 1948.[4] Bloembergen showed on theoretical grounds that reorientation constitutes a major contribution to the relaxation time of the proton spin in NMR experiments on liquid water. The theoretical relationship between the experiment and the underlying orientational (and translational) diffusion of water molecules involves a number of microscopic parameters that are difficult to estimate. Since Bloembergen, the reorientation time τ_r of water (H_2O) has been estimated in NMR experiments with values ranging from 1.7 to 2.8 ps.[41,50,53,55,68,111] This reorientation time decreases with temperature due to the increased thermal energy that is available, in a way that cannot be described by Eq. (7.1), which suggests that it is an activated process that might be

described by the Arrhenius equation

$$\frac{1}{\tau_r(T)} = \frac{1}{\tau_{r,o}} e^{-E_{act}/k_B T}, \tag{7.3}$$

where E_{act} is the activation energy. However, the observed temperature dependence of τ_r shows a small, but significant deviation from a pure Arrhenius behavior. The temperature dependence is described more accurately by the fractional power law[50,104]

$$\frac{1}{\tau_r(T)} \propto (T/T_s - 1)^{\gamma}, \tag{7.4}$$

where $T_s \approx 228$ K and $\gamma \approx 1.78$, which is equivalent to an activation energy that decreases with increasing temperature. Equation (7.4) was originally based on measurements of thermodynamic properties such as the isothermal compressibility and the density, that can all be described by the same critical temperature $T_s = 228\ K$.[112] In NMR, reorientation on a picosecond timescale results in a proton spin relaxation time that is on the order of seconds. It is clear that such a measurement concerns the average reorientation time over long timespans. It does not provide information on whether the orientational motion of a water molecule is truly a diffusive process, or occurs in relatively large jumps.

More recently, experimental techniques became available that act on a timescale comparable to the reorientation time, contrary to the relatively low frequencies (10^8–10^9 Hz) employed in NMR and older dielectric measurements. For example, Eq. (7.2) has been applied to measurements at THz frequencies, where the oscillation period of the electric field is comparable to the Debye time. These measurements showed that water has actually *two* simultaneous Debye processes, with time constants τ_1 of 8 and 0.2 ps.[57] The time constant of the slower component has a temperature depencence satisfying Eq. (7.4).[104,103] This two-component structure was also observed in optical Kerr effect studies, with time constants of 0.5 and 1.7 ps.[16,96] However, it was not clear to what structural relaxation processes, amongst them reorientation, these time constants exactly apply. More recently, similar experiments did show an orientational decay with $\tau_r = 0.9$ and 3 ps.[128]

Pump–probe experiments on the OH stretch vibration make it possible to directly follow the reorientation of water molecules in time. Moreover, it is possible to probe selectively those molecules with either strong or weak hydrogen bonds. The first experiments of this kind on water employed 250 fs pulses and showed distinct time constants τ_r of 700 fs and 13 ps.[132] The component with the shorter time constant was predominantly visible at the high-frequency side (3500 cm^{-1}) of the OH stretch absorption band, and was completely absent at the low-frequency side of the absorption band. In another recent study, it was found that the reorientational time constant varied from 3.0(1.5) ps at 3500 cm^{-1} to 13(5) ps at 3330 cm^{-1}.[67] In this study, however, 2 ps pulses were employed, which renders the determination of short time constants more difficult.

It must be noted that different experimental techniques act on different orientation vectors **e** with respect to the molecule frame. In pump–probe experiments on the OH stretch vibration, as in this thesis, **e** coincides with the O–H bond in an HDO molecule. In proton-NMR experiments, **e** is the HH vector of a water molecule. Dielectric relaxation measurements refer to the dipole moment vector of an H_2O molecule. The orientational diffusion constants for these vectors may differ slightly from each other; they correspond to the eigenvalues of the orientational diffusion tensor.[138]

This chapter presents a detailed study on the orientational motion of HDO molecules in liquid D_2O. We describe the experimental results with a model that includes the effects of spectral relaxation. By varying the temperature, we obtain information on the activation energy that limits the rate of reorientation.

7.2 Experiment

The difference between the experiments described here and in Chapter 4 concerns only the way the data is treated. The experiments were pump–probe measurements where a femtosecond infrared laser pulse excited the $v = 0 \rightarrow 1$ transition of the OH stretch vibration of HDO molecules dissolved in D_2O. The probe pulse has a polarization of 45 deg with respect to the pump pulse polarization; the difference in transmittance between the parallel and perpendicular component enables a measurement of the rotational anisotropy. The general background on pump–probe experiments is discussed in §1.2, the details of the pulse generation in §2.2.3, and the pump–probe setup in §2.4.2.

Directly after excitation, the population of excited molecules per unit of solid angle will be proportional to $\cos^2\theta$, where θ is the angle between the O–H bond and the pump polarization. Due to this anisotropic population of excited molecules, the absorbance changes for probe parallel to pump and perpendicular to pump are different: $\Delta\alpha_{\parallel}/\Delta\alpha_{\perp} > 1$. From $\Delta\alpha_{\parallel}$ and $\Delta\alpha_{\perp}$, we can calculate the rotational anisotropy[44]

$$A = \frac{\Delta\alpha_{\parallel} - \Delta\alpha_{\perp}}{\Delta\alpha_{\parallel} + 2\Delta\alpha_{\perp}}. \tag{7.5}$$

The denominator here corresponds to the isotropic absorbance change, that is not affected by reorientation. For the initial $\cos^2\theta$ distribution, it can be shown that $A = 2/5$. As this highly anisotropic distribution becomes more and more isotropic as a result of reorientation of the individual HDO molecules, the value of A decays to zero with the time constant τ_r (§7.6.1). By measuring A as a function of the delay between pump and probe pulses, we obtain information on the orientational motion of the HDO molecules. See also §2.7.1 for details on evaluating Eq. (7.5) with high accuracy. Note that A is not affected by the relaxation of excited molecules to the ground state, since this affects the numerator and the denominator of Eq. (7.5) in the same way.

The probe and pump pulses have equal frequencies. The sample was a 500 μm-thick layer of a HDO:D_2O solution in a sample cell that was continuously rotated to eliminate local accumulation of heat (§2.8) and that was equipped with a heater that enabled us to control the sample temperature within 1 K.

7.3 Results

Figure 7.1 shows a typical measurement of the transmittance changes $T_\varepsilon/T_\varepsilon^\circ$ and D/D° in HDO:D_2O as a function of the delay between the pump and probe pulses. We repeated these measurements as a function of both the temperature (in the range 298–362 K) and the pulse frequency (3400 and 3500 cm^{-1}).

Due to scattered light from the pump pulses, the data in Fig. 7.1 have a significant background. As is clear from Eq. (7.5), any tiny background contribution has a large

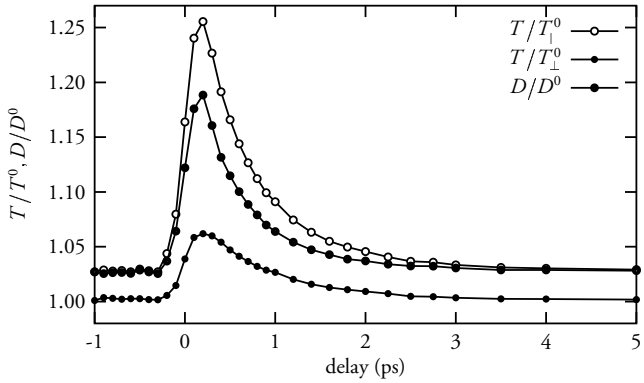

FIGURE 7.1. Raw data of $T_{\parallel}/T^{\circ}_{\parallel}$, $T_{\perp}/T^{\circ}_{\perp}$ and D/D° (see §2.7.1). The frequency was 3400 cm^{-1} and the temperature was 298 K. The different background levels are caused by scattered light from the pump pulses. The smooth increase of the signal around $t = 0$ ps is caused by the nonzero pulse duration.

effect on the value of the rotational anisotropy A. Since the bleaching decays with a time constant of 850 fs (Chapter 4) the residual bleaching at $t = 5$ ps is of the same magnitude as the error in the data points. In order to evaluate the background with the highest possible accuracy, we assumed an exponential decay of the raw T/T° values in Fig. 7.1 in the range 1.5–5 ps. The assumption of exponential decay is justified, since the resulting rotational anisotropy A in Fig. 7.2 decays exponentially for $t > 1.5$ ps.

The data in Fig. 7.2 display several facts. (i) This decay is faster in the experiments at 3500 cm^{-1} than in the experiments at 3400 cm^{-1}. (ii) The decays are not exponential, which is best visible at delay times less than 1.5 ps. (iii) The decay of the rotational anisotropy becomes faster as the temperature increases.

7.4 ACTIVATED REORIENTATION AND SPECTRAL DIFFUSION

7.4.1 MODEL

The frequency dependence of the anisotropy decay suggests that the reorientation rate of an individual molecule depends on its resonance frequency. This can be expected in view of the relation between OH stretch frequency and hydrogen bond strength: a higher OH vibration frequency implies a weaker hydrogen bond,[85,92] which must lead to a larger freedom for the OH group to change its orientation. Since it is likely that, in order to change its orientation, a water molecule must stretch or break the hydrogen bond, this activation energy E_{act} is expected to decrease with increasing OH stretch frequency ω. The reorientation time τ_r should satisfy Eq. (7.3) where E_{act} is replaced by $E_{act}(\omega)$, which results in a frequency-dependent reorientation time $\tau_r(\omega)$. The prefactor $\tau_{r,0}$ is an indication for the reorientation time in absence of any activation energies, i.e. the gas-phase rotation time. For an HDO molecule at 298 K, the classical angular frequency corresponding to a rotational energy of $k_B T$ is approximately 10 ps^{-1}.

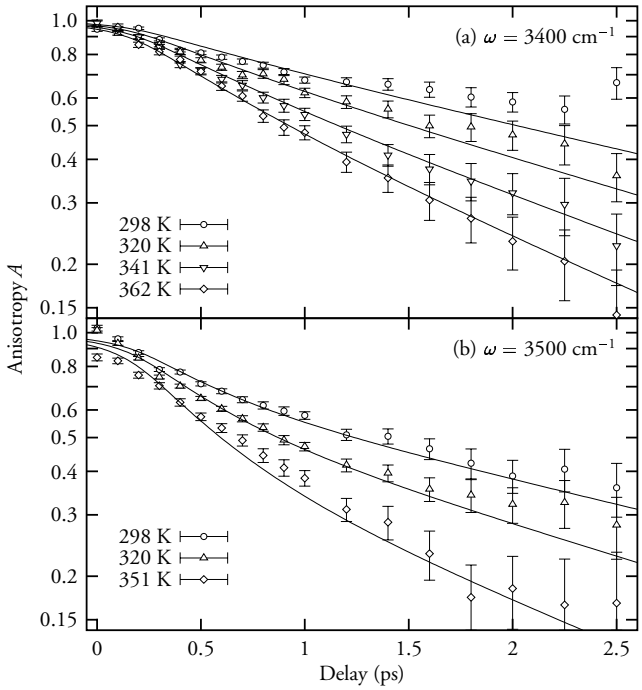

FIGURE 7.2. The decay of the rotational anisotropy A in HDO:D_2O for a series of temperatures, measured at excitation frequencies 3400 and 3500 cm^{-1}. The data are normalized at $t = 9$ ps. The lines represent our model calculations, discussed in §7.4.

A frequency dependence of the reorientation time τ_r cannot provide a complete description of the observed reorientation in water, since the OH stretch frequencies of individual HDO molecules fluctuate rapidly in time. (See also Refs. 33, 129 and Chapter 5.) We must therefore incorporate this spectral diffusion process into our model. We assume that we can describe the spectral diffusion by the Brownian-oscillator model in §5.4.[♩] The spectral diffusion has a correlation time τ_c that is 500 fs according to Ref. 129 or 700 fs according to Ref. 33.

The combination of spectral diffusion and a frequency-dependent reorientation rate is too complicated for an analytical treatment such as in Eq. (5.4). Therefore, we used numerical methods to evaluate the reorientational dynamics. The absorbance changes in Eq. (7.5) depend on the difference in population of the vibrational ground and excited state before and after the pump pulse. Equation (1.3) described the absorbance change for a probe polarization ε, which depends on the orientational distribution parameter ξ_ε. Due to the Stokes shift, the spectral relaxation of the n_0 population differs from that of the n_1 population. Hence, we refine Eq. (1.3) to account for the different frequency- and time-dependent contributions of the ground-state depletion $-\Delta n_0(\omega, t)$ and the excited-state

[♩] Section 5.4 discusses the spectral relaxation of the OD stretch vibration. It applies to the present chapter up to Eq. (5.3), if one reads 'OH' for every occurence of 'OD'.

population $\Delta n_1(\omega, t)$, which gives us

$$\Delta\alpha_\varepsilon(\omega,t) = \bar{\sigma} e^{-t/T_1}\big[\Delta n_0(\omega,t)\xi_{0,\varepsilon}(\omega,t) + \Delta n_1(\omega,t)\xi_{1,\varepsilon}(\omega,t)\big], \tag{7.6}$$

where $\bar{\sigma}$ defines the amplitude of the bleaching [see also Eq. (1.6)]. If we take the spectrum and duration of the probe pulse into account, we can write the measured rotational anisotropy as

$$A(t) = \frac{\int I_{\text{probe}}(\omega,t) * \big[\Delta\alpha_{\parallel}(\omega,t) - \Delta\alpha_{\perp}(\omega,t)\big]\,d\omega}{\int I_{\text{probe}}(\omega,t) * \big[\Delta\alpha_{\parallel}(\omega,t) + 2\Delta\alpha_{\perp}(\omega,t)\big]\,d\omega}, \tag{7.7}$$

where $I_{\text{probe}}(\omega, t)$ is the power spectrum of the probe pulses at time t and the $*$ operator indicates time convolution. For the analysis, it is more convenient to write

$$\Delta\alpha_{\parallel}(\omega,t) - \Delta\alpha_{\perp}(\omega,t) = \bar{\sigma}\big[a_-(\omega,t) + b_-(\omega,t)\big], \tag{7.8A}$$
$$\Delta\alpha_{\parallel}(\omega,t) + 2\Delta\alpha_{\perp}(\omega,t) = \bar{\sigma}\big[a_+(\omega,t) + b_+(\omega,t)\big], \tag{7.8B}$$

where $a_\pm$ and $b_\pm$ are defined as

$$a_-(\omega,t) = \Delta n_0(\omega,t)\big[\xi_{0,\parallel}(\omega,t) - \xi_{0,\perp}(\omega,t)\big], \tag{7.9A}$$
$$b_-(\omega,t) = \Delta n_1(\omega,t)\big[\xi_{1,\parallel}(\omega,t) - \xi_{1,\perp}(\omega,t)\big], \tag{7.9B}$$
$$a_+(\omega,t) = \Delta n_0(\omega,t)\big[\xi_{0,\parallel}(\omega,t) + 2\xi_{0,\perp}(\omega,t)\big], \tag{7.9C}$$
$$b_+(\omega,t) = \Delta n_1(\omega,t)\big[\xi_{1,\parallel}(\omega,t) + 2\xi_{1,\perp}(\omega,t)\big]. \tag{7.9D}$$

The excitation by the pump pulse, spectral diffusion, and reorientation, affect $a_\pm$ and $b_\pm$ according to the partial differential equations

$$\frac{\partial a_-}{\partial t} = \frac{2}{5} I_{\text{pump}}(\omega,t) + \mathcal{D}_0 a_- - \frac{a_-}{\tau_r(\omega)}, \tag{7.10A}$$
$$\frac{\partial b_-}{\partial t} = \frac{2}{5} I_{\text{pump}}(\omega,t) + \mathcal{D}_1 b_- - \frac{b_-}{\tau_r(\omega)}, \tag{7.10B}$$
$$\frac{\partial a_+}{\partial t} = I_{\text{pump}}(\omega,t) + \mathcal{D}_0 a_+, \tag{7.10C}$$
$$\frac{\partial b_+}{\partial t} = I_{\text{pump}}(\omega,t) + \mathcal{D}_1 b_+. \tag{7.10D}$$

Here, $I_{\text{pump}}(\omega, t)$ is the normalized pump intensity (the absolute magnitude is not relevant, since this does not affect the value of A). The operators $\mathcal{D}_0$ and $\mathcal{D}_1$ act on ω and describe spectral diffusion in the $v = 0$ and $v = 1$ states (See §7.6.2 for details). The coefficient $2/5$ in Eqs. (7.10a–b) ensures that the initial anisotropy is $2/5$ in absence of spectral diffusion and orientational relaxation. Equations (7.10) are integrated numerically. Using the solutions of Eqs. (7.10), we calculate the decay of the measured anisotropy A in Eq. (7.7). We find that the experimental data can be well described if the activation energy E_{act} depends on the frequency as

$$E_{\text{act}}(\omega) = \begin{cases} 600 + 1.81(3675 - \omega) & (\omega \le 3675) \\ 600 & (\omega \ge 3675) \end{cases}, \tag{7.11}$$

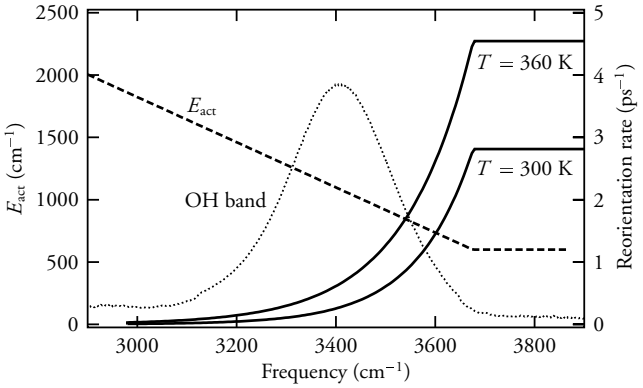

FIGURE 7.3. Reorientation rate, defined as $1/\tau_r$, at 300 and 360 K (solid lines, right-hand scale), the rotational activation energy as a function of the OH stretch frequency (dashed line, left-hand scale), and the shape of the OH absorption band (dotted line). To convert cm^{-1} to J/mol, multiply by 11.96.

where E_{act} and ω are expressed in cm^{-1} units.[♩] The constant of 600 cm^{-1} corresponds to the activation energy caused by effects such as steric hindering and other hydrogen bonds that do not affect the OH stretch frequency. The 3675 cm^{-1} cut-off frequency is approximately equal to the gas-phase frequency where no DO–H$\cdots$O hydrogen bond is present. Furthermore, the pre-exponential time constant is $\tau_{r,0} = 20$ fs, which is of the same order as the thermal rotation time of 100 fs in the gas phase.

The resulting frequency and temperature dependence of the reorientation rate in Fig. 7.3 increases rather steeply. It is not possible to describe the experimental results with a smoother frequency dependence of the reorientation rate. Further, we describe the spectral diffusion with a 60 cm^{-1} Stokes redshift and a spectral correlation time $\tau_c = 500$ fs, in agreement with earlier results.[129] The resulting decays of the anisotropy are shown in Fig. 7.2.

7.4.2 DISCUSSION OF THE MODEL

For very small delays ($t < 0.2$ ps), the anisotropy decays more slowly than at larger delays, both in the calculations and the experiment. This is simply due to the fact that for these small delays, the creation of 'new anisotropy' by the pump pulse compensates the decay of anisotropy due to reorientation. In addition, it can be expected that during the temporal overlap between pump and probe pulses around $t = 0$ ps, coherent coupling effects cause a small additional contribution to the anisotropy signal. Although there appears to be no coherent peak in the anisotropy, we did not draw definite conclusions about the reorientation from the data around zero delay.

At delays <1.5 ps, the anisotropy decay depends strongly on frequency. At 3500 cm^{-1}, most excited molecules will initially be in the fast-reorienting part of the spectrum and thus cause a relatively high anisotropy decay rate. At 3400 cm^{-1}, the initial decay rate is only

[♩] To obtain an activation energy in J/mol, replace the numbers 600 and 1.81 by 7176 and 21.6, respectively

TABLE 7.1. Reorientation times after equilibration of the transient spectrum for the $v = 0$ and $v = 1$ vibrational states, calculated from the model. The values for $\tau_{r,eq}(v = 0)$ correspond to the reorientation times of water molecules in the absence of excitation by laser pulses.

T (K)	$\tau_{r,eq}(v = 0)$ (ps)	$\tau_{r,eq}(v = 1)$ (ps)
298	2.59	4.16
320	1.98	3.04
341	1.59	2.36
351	1.45	2.12
361	1.32	1.90

slightly faster than the average decay rate that is effective at larger delays (i.e. $t > 1.5$ ps). At these larger delays, the absolute value of the anisotropy is systematically lower at the high-frequency. However, the anisotropy decay rate does not depend on the frequency at these larger delay times (See §7.6.3 for the proof). This final decay rate depends on the spectral relaxation constant, the fraction of molecules with a large reorientation rate, and the maximum value of the reorientation rate at the high-frequency side of the spectrum (which increases with temperature). This final decay of the anisotropy is determined by both the anisotropy decay of the $v = 0$ state and that of the $v = 1$ state. The fraction of fast-reorienting molecules in the $v = 1$ state [the $b_{\pm}$ components in Eqs. (7.8)] is smaller than the fraction of fast-reorienting molecules in the $v = 0$ state (the $a_{\pm}$ components), due to the Stokes redshift in the $v = 1$ spectrum. This results in slightly different anisotropy decay rates for these two contributions to the anisotropy signal.

To summarize, there are three time constants that contribute to the anisotropy decay at a given frequency and temperature. The first time constant is the inverse of the reorientation rate at the excitation frequency; it mainly affects the decay at smaller delays. The value for this time constant can be read from Fig. 7.3. The second and the third time constants $\tau_{r,eq}(v = 0)$ and $\tau_{r,eq}(v = 1)$, that determine the decay at larger delays, are the reorientation time constants for the $v = 0$ and $v = 1$ states, respectively, after equilibration of the shape of the transient spectrum. By calculating the a and b contributions in Eq. (7.8) separately, we found the time constants for these slow processes as shown in Table 7.1. From Fig. 7.3, it is clear that only OH groups with a weak hydrogen bond are able to change orientation. This implies that a molecule with a low OH frequency and a strong hydrogen bond can only change orientation if the hydrogen bond is temporarily stretched, which corresponds to spectral diffusion to higher frequencies. In other words, only spectral diffusion enables low-frequency molecules to change their orientation.

In our model, we have used the 500 fs time constant for spectral relaxation from Ref. 129. However, it is possible to describe our data with the 700 fs time constant measured by Gale et al.[33] In that case, we find a slightly different activation energy, resulting in a reorientation rate curve in Fig. 7.3 that is shifted towards lower frequencies by less than 10 cm^{-1}. This shows that the model is not extremely sensitive to the spectral relaxation time constant.

Although our model can account well for both the frequency and the temperature dependence of the anisotropy decay, some refinements of the model are still possible. First, it is known that the OH stretch absorbance line shape changes with temperature.[28]

In principle, this could be accounted for by modifying the spectral diffusion operators in Eqs. (7.10). Second, we assume that there is a single, well-defined, activation energy at a given OH stretch frequency. However, this activation energy may very well depend on the strength of the other hydrogen bonds to other neighboring water molecules. Therefore, it would be more correct to assume a distribution of activation energies (and a resulting distribution of reorientation rates) at each frequency. Finally, in our model we explicitly account for the fact that the reorientation of the water molecules is enabled by the spectral diffusion. However, we do not take into account that in turn the spectral diffusion may be affected by the reorientation. When an OH group changes its orientation, it is likely that the length of its hydrogen bond will change simultaneously. In other words, reorientation by itself contributes to spectral diffusion. In principle, the model could be refined by assuming that the spectral diffusion time constant has a frequency-dependence that is linked to the reorientation time constant, e.g. $1/\tau_c(\omega) = 1/\tau_{\min} + K/\tau_r(\omega)$, where $\tau_{\min}$ and K are to be determined from our data. However, this refinement will have little effect, since at lower frequencies, the reorientation takes place on a much slower time scale than the spectral diffusion, whereas at high frequencies, the hydrogen-bond length is large and any rotations will not strongly influence the frequency of an OH vibration. In addition, the spectral relaxation in water can be well described as a Gauss-Markov process, as was shown by Woutersen and Bakker[129] and Gale et al.[33] We will discuss this in more detail in Chapter 8. This means that there is no evidence for a significant frequency dependence of spectral diffusion.

7.4.3 Comparison with other studies

In a previous publication,[132] time constants τ_r of 0.7 and 13 ps were obtained with the same method as presented here. The 0.7 ps time constant corresponds to a spectral average of the initial fast process at the high-frequency side of the spectrum (approximately 1 ps), while the 13 ps time constant corresponds to the slower time constants $\tau_{r,eq}(v = 0) = 2.6$ ps and $\tau_{r,eq}(v = 1) = 4.2$ ps that result after equilibration of the transient spectral line shapes. The time constants differ from the earlier results due to the improved signal-to-noise ratio.

The reorientational dynamics of liquid water have also been investigated with molecular dynamics simulations. These calculations yield time constants that depend strongly on the simulation method. In *ab initio* density functional theory calculations, values for τ_2 have been reported that range from 1.2 to 9 ps.[113] In classical molecular dynamics studies, time constants between 0.7 and 1.7 ps were found.[15,122] In one study, a bi-exponential decay of $C_2(t)$ was found with 1.0 and 13 ps time constants.[137]

According to NMR experiments,[105] the reorientation time τ_r of HDO in D_2O decreases from 2.7 ps at 298 K to 0.81 ps at 350 K.♪ These values are slightly smaller than those for $\tau_{r,eq}(v = 0)$ in Table 7.1. In both H_2O and D_2O, the Debye time τ_1 varies from approximately 8 ps at 300 K to 3 ps at 360 K, with a small isotopic effect.[57,103,104] These values correspond to $\tau_r = 2.7$ and 1.0 ps, respectively. Interestingly, the reorientation time $\tau_{r,eq}(v = 0)$ in Table 7.1 satisfies Eq. (7.3) with $E_{act} = 1147$ cm^{-1} (13.7 kJ/mol) and $\tau_{r,0} = 55$ fs. Hence, the model discussed in this chapter does not show the behavior of Eq. (7.4), which predicts a activation energy that decreases with increasing temperature. Two things must be noted. (i) The present model does not take into account that the OH

♪ Isotopic correction factors from Refs. 68 and 50 were applied to obtain numbers for HDO in D_2O.

absorption band of HDO:D_2O shifts towards higher frequencies with increasing temperature due to a weakening of the hydrogen bonds.[28] In the present context, the OH band in Fig. 7.3 shifts to the right, which corresponds to an overall lower rotational activation energy. (ii) In the temperature range of the present study, the critical temperature equation, Eq. (7.4), differs by less than a fraction 0.02 from a pure Arrhenius-like behavior [Eq. (7.3)]. Hence, the time constants found in NMR and dielectric relaxation measurements are in agreement with the value of $\tau_{r,eq}(v = 0)$ that we observe after the transient spectrum has equilibrated. This $\tau_{r,eq}(v = 0)$ represents an effective reorientation time scale that forms an average over *all* water molecules. An important advantage of the femtosecond nonlinear spectroscopic method employed in this work is that the reorientational dynamics of a *subensemble* of the water molecules can be investigated. This enables a determination of the mechanism behind the effective reorientation time of liquid water as observed in NMR and dielectric relaxation experiments. This work shows that the effective reorientation rate in liquid water is governed by the fraction of water molecules for which reorientation is not hindered by the OH$\cdots$O hydrogen bond, the rate of this unhindered reorientation, and the rate at which the strength of the hydrogen bonds is stochastically modulated.

7.5 Conclusions

We have measured the orientational relaxation of HDO molecules dissolved in liquid D_2O by creating an anisotropic population of excited OH stretch vibrations with femtosecond mid-infrared pulses and by subsequently measuring the decay of this anisotropy. The decay of the anisotropy is nonexponential and takes place on a typical time scale of 1 ps. At the blue side of the inhomogeneously broadened OH stretch vibration absorption band (3500 cm^{-1}), the anisotropy decays faster than at the center of the absorption band (3400 cm^{-1}).

We find that the frequency and temperature dependence of the anisotropy decay can be well described with a model in which the reorientation is an activated process. The activation energy for reorientation decreases linearly with increasing hydrogen-bond length. This yields a reorientation rate as a function of frequency that increases steeply. By varying the temperature, we find that the maximum reorientation rate at the high-frequency side of the absorption band increases from 2.8 ps^{-1} at 298 K to 4.5 ps^{-1} at 360 K.

The model also includes the effects of spectral diffusion that results from the stochastic modulation of the hydrogen-bond length. It is found that the reorientation of strongly hydrogen-bonded water molecules is enabled by the weakening of the hydrogen bond.

7.6 Appendix: mathematical details

7.6.1 Rotational diffusion

Orientational diffusion describes the time dependence of the orientation vectors $\mathbf{e}$ of an ensemble of molecules. The vector $\mathbf{e}$ is fixed in the molecular frame and has a time-dependent angular distribution in the laboratory frame $\psi(\theta, \phi, t)$, which represents the

number of particles in a solid angle $d\Omega = \sin\theta\, d\theta\, d\phi$. Its time evolution is described by

$$\frac{\partial}{\partial t}\psi(\theta,\phi,t) = D_{\mathrm{r}}\mathcal{R}\psi(\theta,\phi,t), \tag{7.12}$$

where D_{r} is the rotational diffusion constant and $\mathcal{R}$ is the Laplace operator in polar coordinates,

$$\mathcal{R} = \frac{1}{\sin\theta}\left(\cos\theta\frac{\partial}{\partial\theta} + \sin\theta\frac{\partial^2}{\partial\theta^2} + \frac{1}{\sin^2\theta}\frac{\partial^2}{\partial\phi^2}\right). \tag{7.13}$$

We can construct the solutions of Eq. (7.12) by noting that $\mathcal{R}$ has the spherical harmonics $Y_{lm}(\theta,\phi)$ as eigenfunctions,[54] that have eigenvalues $-l(l+1)$ with $l = 0, 1, 2, \cdots$. The generic solution of Eq. (7.12) is therefore an expansion in eigenfunctions,

$$\psi(\theta,\phi,t) = \sum_{l\geq 0}\sum_{m=-l}^{l} c_{lm}Y_{lm}(\theta,\phi)e^{-D_{\mathrm{r}}l(l+1)t}, \tag{7.14}$$

where c_{lm} are arbitrary constants. In experimental geometries, there is usually no ϕ dependence, which means that $m = 0$ and

$$\psi(\theta,\phi,t) = \sum_{l\geq 0} c_l P_l(\cos\theta)e^{-D_{\mathrm{r}}l(l+1)t}, \tag{7.15}$$

where $P_l(x)$ are Legendre polynomials [i.e., $P_0(x) = 1$, $P_1(x) = x$, $P_2(x) = (3x^2-1)/2$]. It can be shown that the rotational anisotropy $A = \langle P_2(\cos\theta)\rangle$, with $\theta = 0$ corresponding to the pump pulse polarization. Due to the orthogonality of the Legendre polynomials, A decays with a time constant $\tau_{\mathrm{r}} = \tau_2 = 1/6D_{\mathrm{r}}$. The subscript 2 indicates that $l = 2$. The time constants obtained in NMR measurements also refer to τ_2. However, the Debye time obtained in dielectric relaxation measurements corresponds to $\tau_1 = 3\tau_2$.

7.6.2 Spectral diffusion

The operators $\mathcal{D}_v$ originate from the Brownian oscillator model in §5.4, that describes diffusion in a harmonic potential and the resulting spectral diffusion. The equations in §5.4 are a limiting case of the original description in a more general but highly complicated formalism.[88] For the purposes in this chapter and Chapter 8, it is more convenient to treat the Brownian oscillator as a diffusion problem.

A time-dependent distribution $n(R,t)$ of diffusing particles in a potential $W(R)$ satisfies the diffusion equation[63]

$$\frac{\partial n}{\partial t} = D_R\left(\frac{\partial^2}{\partial R^2} + \beta\frac{dW}{dR}\frac{\partial}{\partial R} + \beta\frac{d^2W}{dR^2}\right)n, \tag{7.16}$$

where $\beta = 1/k_{\mathrm{B}}T$ and D_R is the diffusion constant. If we assume a harmonic potential $W_v(R)$ for vibrational state v, we can write

$$D_R = \frac{\tilde{\Delta}^2}{\tau_{\mathrm{c}}}, \tag{7.17}$$

where $\tilde{\Delta}$ is the RMS deviation of R from its central value R_0, or

$$W_0(R_0 \pm \tilde{\Delta}) - W_0(R_0) = k_B T/2. \tag{7.18}$$

With the potentials for the $v = 0$ and $v = 1$ states in Fig. 5.3, we can use Eq. (7.16) to obtain the diffusion equation

$$\frac{\partial a}{\partial t} = \mathcal{D}_0 a, \tag{7.19}$$

which is in terms of the spectral response $a(\omega, t)$ of the bleaching contribution of the $v = 0$ state (i.e. the B_{01} contribution in Eq. (5.4) before convolution with the spectrum of the probe pulses), where

$$\mathcal{D}_0 = \frac{1}{\tau_c}\left(\Delta_d^2 \frac{\partial^2}{\partial \omega^2} + (\omega - \omega_B)\frac{\partial}{\partial \omega} + 1\right). \tag{7.20}$$

Here, Δ_d is the standard deviation of the Gaussian linear absorption spectrum, centered at $\omega = \omega_B$, that results from the parabolic potentials $V_v(R)$. The operator $\mathcal{D}_1$ for the bleaching contribution $b(\omega, t)$ of the $v = 1$ state (similar to B_{10} in Eq. (5.4)) is very similar, i.e.

$$\mathcal{D}_1 = \frac{1}{\tau_c}\left(\Delta_d^2 \frac{\partial^2}{\partial \omega^2} + (\omega - \omega_B + \delta\omega_{sto})\frac{\partial}{\partial \omega} + 1\right), \tag{7.21}$$

where $\delta\omega_{sto}$ is the Stokes shift.

7.6.3 Anisotropy decay at large delays

It is relatively easy to see that the anisotropy A decays exponentially at large delays. Similar to the rotational-diffusion operator in §7.6.1, the spectral-diffusion operator $\mathcal{D}_0$ has eigenfunctions $\phi_j(\omega)$ with eigenvalues λ_j. All eigenvalues are negative, except for $\lambda_0 = 0$, which corresponds to the distribution in thermal equilibrium. Thus, the isotropic signal [see Eq. (7.10c)], for delays t much larger than the pulse duration, has the general form

$$a_+(\omega, t) = c_0\phi_0(\omega) + \sum_{j\geq 1} c_j \phi_j e^{\lambda_j t}. \tag{7.22}$$

The anisotropic signal a_- has a different set of eigenfunctions $\chi_j(\omega)$ with eigenvalues μ_j, which are all negative due to the loss term in Eq. (7.10a); its expansion is

$$a_-(\omega, t) = \sum_{j\geq 1} d_j \chi_j e^{\mu_j t}. \tag{7.23}$$

If we define k as the index for the largest eigenvalue μ_k, the rotational anisotropy $A_0 = a_-/a_+$ for the ground state contributions will approach

$$A_0(t) \to d_k e^{\mu_k t}/c_0 \tag{7.24}$$

asymptotically for $t \gg \tau_c$. The coefficients d_k and c_0 depend on the initial distributions of $a_\pm$ (that depend on the pump pulse spectrum), but the decay rate $\mu_k = -1/\tau_{r,eq}(v = 0)$ is independent on these initial distributions. Similar arguments apply to the overall anisotropy A in Eq. (7.7).

7.6.4 Numerical implementation

Calculating the time-evolution of the diffusion equation (7.16) can be done with a forward time centered space (FTCS) algorithm.[100] If a function $f(R)$ (representing either V or n) is discretized as f_i with steps δR, then derivatives to R can be approximated as

$$f_i' \equiv \frac{\partial f}{\partial R} \approx \frac{1}{2\delta R}(f_{i+1} - f_{i-1}), \tag{7.25}$$

$$f_i'' \equiv \frac{\partial^2 f}{\partial R^2} \approx \frac{1}{\delta R^2}(f_{i+1} + f_{i-1} - 2f_i). \tag{7.26}$$

For numerically stable behavior, it is usually sufficient to set

$$\delta t = (1 - \epsilon)\delta R^2/2D_R, \tag{7.27}$$

with $\epsilon \approx 0.1$. The diffusion equations for the $v = 0$ and $v = 1$ vibrational states should be solved independently from each other yielding solutions $n_0(R)$ and $n_1(R)$. The spectral response, including the induced absorption due to the $v = 1 \to 2$ transition, is

$$a(\omega) = \left[n_0(R_{01}(\omega)) + n_1(R_{01}(\omega))\right]\frac{dR_{01}}{d\omega} - \sigma n_1(R_{12}(\omega))\frac{dR_{12}}{d\omega} \tag{7.28}$$

where σ is the relative cross-section of the $v = 1 \to 2$ transition and $R_{jk}(\omega)$ are mappings of the $v = j \to k$ transition frequency to R, i.e. the inverse functions of

$$\omega_{jk}(R) = V_k(R) - V_j(R), \tag{7.29}$$

where we assume $\hbar = 1$. If i has a finite range $0 \cdots N - 1$, boundary conditions can be implemented by assuming $n_0 = n_{N-1} = 0$; after each timestep, add the new value n_0 to n_1 and add the new value n_{N-1} to n_{N-2}.

Equation (7.20) is useful if harmonic potentials can be assumed and no contribution of the $v = 1 \to 2$ transition is used. The former is the case in this chapter. To conserve the number of particals upon numerical integration, the factor $(\omega - \omega_B)$ in Eq. (7.20) should be written as the numerical approximation of $d\left[(\omega - \omega_B)^2/2\right]/d\omega$ and not as $\omega - \omega_B$.